Alkyl-modified oligonucleotides as intercalating vehicles for doxorubicin uptake via albumin binding.

Laura Purdie,† Cameron Alexander,† Sebastian G. Spain,‡ and Johannes P. Magnusson†**

† School of Pharmacy, University of Nottingham, University Park, Nottingham, UK. NG7 2RD.

‡ Department of Chemistry, University of Sheffield, Sheffield, UK. S3 7HF.

KEYWORDS : Oligonucleotides, Albumin, Cytotoxic, Prodrug. Mitochondrial targeting

ABSTRACT

DNA-based drug delivery vehicles have displayed promise for the delivery of intercalating drugs. Here, we demonstrate that oligonucleotides modified with an alkyl chain can bind to human serum albumin, mimicking the natural binding of fatty acids. These alkyl-DNA-albumin complexes display excellent serum stability and are capable of strongly binding doxorubicin. Complexes are internalized by cells *in vitro,* trafficking to the mitochondria, and are capable of delivering doxorubicin with excellent efficiency resulting in cell death. However, the cellular localization of the delivered doxorubicin, and ultimately the complex efficacy, is dependent on the nature of the linker between the alkyl group and the oligonucleotide.

INTRODUCTION

Nature has evolved highly efficient transport processes for regulating nutrients, waste products and exogenous compounds to maintain homeostasis within the human body.[1] New therapeutics therefore often require optimization to ensure a positive clinical outcome. For example, pharmacokinetics may be enhanced by derivatization of the therapeutic or incorporation into synthetic carriers such as micelles, nanoparticles and liposomes.[2–4] Natural particulates such as viruses and proteins are of increasing interest as delivery platforms for biologics and small drugs since they have the ability to pass through cell barriers, evade clearance by the body and often have an established pharmacokinetic profile.[5–7] Human serum albumin (HSA) has been extensively studied and developed as a delivery platform towards this end with albumin-binding formulations such as Abraxane (HSA-bound paclitaxel) and Levemir (Myristic acid insulin conjugate) already in the clinic and Aldoxorubicin (HSA-bound doxorubicin) in Phase III clinical trials for soft tissue sarcoma.[8] Albumin has favourable properties for therapeutic optimization including a long half-life, high abundance in plasma, a well-defined structure, and excellent binding properties for both endogenous and exogenous compounds.[9–12] Albumin is also of increasing importance for the delivery of cytotoxics since its uptake and metabolism is upregulated in tumor cells[13–15] and its accumulation in tumor neo-vasculature by the Enhanced Permeation Retention (EPR) effect.[16,17]

The ability of intercalating cytotoxics to form strong physical complexes with double stranded oligonucleotides (dsODN)[18] has been studied as a potential prodrug strategy in oncology. [19,20] However, poor stability and low cellular uptake of oligonucleotides *in vivo* still provide a major barrier clinical translation. Recent developments in nucleoside chemistry and the assembly of highly elaborate DNA structures at the nanoscale have come some way in addressing these

issues.[21] However, these approaches need to be simplified to facilitate scale-up and minimize the potential cost of therapy.[22–25]

We have previously investigated the effects of polymer conjugation to both 5' ends of a 22mer dsODN and the effects on delivery of the intercalating cytotoxic doxorubicin.[20] The PEG conjugation was found not to affect dsODN-drug affinity while significantly improving the stability of the dsODN against nucleases. However, PEGylated dsODNs were found to be less effective than free doxorubicin and were unable to enhance sensitivity of a drug resistant cell line.

Herein, we describe a pro-drug inspired by the ability of albumin to transport fatty acids into cells to deliver doxorubicin using an alkylated dsODN as a fatty acid mimic (Figure 1a). The dsODNs were modified with alkyl chains of various lengths and functionalities which were screened and selected on the merit of their albumin binding. The best candidates were evaluated *in vitro* in terms of stability, dsODN cellular uptake and doxorubicin delivery. The linker design played a pivotal role in determining albumin binding, stability and cellular uptake of the carrier with the introduction of a small spacer between the alkyl and dsODN chains affecting albumin binding, stability, cellular uptake and the ultimate cytotoxicity of a doxorubicin-loaded conjugates. A selected alkyl-dsODN conjugate demonstrated rapid uptake of the dsODN carrier and intracellular doxorubicin levels which were comparable to that of the free drug.

MATERIALS AND METHODS

Oligonucleotides (HPLC purified) were purchased from Biomers.net GmbH (Ulm, Germany) and used without further purification. Oregon Green® 488 Carboxylic Acid, Succinimidyl Ester, 5-isomer was purchased from Life Technologies. PD SpinTrap G-25 columns, Disposable PD-10 Desalting Columns, Biacore CM5 sensor chip and HBS-P buffer were purchased from GE

Healthcare Life Sciences. All solvents and reagents were of analytical or HPLC grade and purchased from Sigma Aldrich unless otherwise specified. *N*,*N*'–Disuccinimidyl carbonate (DSC, ≥95.0%), triethylamine (Et_3N, ≥99%), water (BPC grade), diammonium hydrogen citrate (DAHC, ≥99%), 3-hydroxypicolinic acid (3-HPA, ≥99%), methylene blue hydrate (>97%), tris-borate-EDTA buffer (TBE, 10× concentrate), ammonium persulfate (≥98%), *N*,*N*,*N*′,*N*′-tetramethylethylenediamine (TEMED, 99%), ethylenediaminetetraacetic acid disodium salt (EDTA, >99%), glycerol anhydrous (Fluka), 1-octadecanol (99%), 1-tetradecanol (97%), Oleyl alcohol (>99%), 1-Hexanol (99%), 2-(2-Aminoethoxy)ethanol (98%), Tetrahydrofuran (THF) anhydrous, bromophenol blue solution (0.04 wt% in H_2O), acrylamide:*N*,*N*′-methylenebisacrylamide (29:1) 40% solution, fetal calf serum (FCS) and Dulbecco's phosphate-buffered saline (modified, without calcium chloride and magnesium chloride) were purchased from Sigma Aldrich.

NMR spectroscopy

NMR spectra were recorded on a Bruker Avance 400 spectrometer at 399.8 MHz (^1H) and 100.5 MHz (^{13}C) in d-chloroform unless otherwise stated. All chemical shifts are reported in ppm relative to TMS. ^1H NMR spectra are available in the ESI.

SEC analysis, HPLC analysis and purification of DNA strands

Size exclusion chromatography (SEC) and reverse phase high performance liquid chromatography (RP-HPLC) was performed on a Shimadzu Prominence UPLC system fitted with a DGU-20A5 degasser, LC-20AD low-pressure gradient pump, CBM-20A LITE system controller, SIL-20A autosampler, an SPD-M20A diode array detector and RF-10AXL fluorescence detector.

RP-HPLC: Analytical separations were performed on a Phenomenex Clarity 3 μm Oligo-RP C18 column (4.6 × 50 mm) using a gradient of 10-70% MeOH over 20 min with an 80% MeOH wash step in 0.1 M triethylammonium acetate (TEAA, pH 7.5)/MeCN (95/5) at a flow rate of 1.0 mL/min. Semi-preparative separations were performed on a Phenomenex Clarity 3 μm Oligo-RP C18 column (10 × 50 mm) under the same conditions at a flow rate of 4.5 mL/min.

SEC: Protein-dsODN competitive binding was performed in isotonic PBS pH 7.4 (Dulbecco) using a TSKgel G3000SWXL (TOSOH) column at 1 mL/min. UV absorbance was recorded at 220 nm.

MALDI analysis

Matrix-assisted laser desorption/ionization time-of flight (MALDI-TOF) mass spectrometry was performed on a Bruker MALDI-TOF Ultra Flex III spectrometer operated in reflective, negative ion mode. 3-HPA containing DAHC was used as the matrix for oligonucleotide analysis. Briefly, a saturated solution of 3-HPA (50 mg/mL) was prepared by adding 25 μg of 3-HPA to 500 μL of 50% ACN/water. 25 μL of DAHC solution (100 mg/mL) was added to 225 μL of the 3-HPA solution, to give a final DAHC concentration of 10 mg/mL. Equal volumes of matrix solution and ODN solution (0.2 mM) were mixed and 2 μL of the mixture was spotted onto the MALDI plate and allowed to dry.

Synthesis of octadecanol-DSC (C18-DSC)

1-Octadecanol (5 g, 0.0184 mol) was weighed out and placed in a sealed round bottom flask. The lipid was dissolved in anhydrous THF (100 mL) and the solution cooled down to 0°C in an ice bath. DSC (9.47 g, 0.0369 mol) and Et_3N (4.67 g, 0.046 mol) were added to the solution which was allowed to warm to room temperature (ca. 20 °C) and then left to react overnight (16 h.). The resulting suspension was filtered to remove solids and volatiles were removed under

reduced pressure. The yellowish powder residue was dissolved in a minimal amount of DCM and the product was precipitated from methanol. The precipitation was repeated twice to give the C18-DSC as a white powder (5.30 g, 70% yield).

^{1}H NMR ($CDCl_3$, 400 MHz): δ 4.33-4.28 (t, 2H), 2.83 (s, 4H), 1.78-1.70 (m, 2H), 1.43-1.18 (m, 30H), 0.90-0.85 (t, 3H). ^{13}C NMR ($CDCl_3$, 100 MHz): δ 168.65, 151.60, 71.68, 31.92-28.37 (multiple signals), 25.46, 25.42, 22.68, 14.11.

Synthesis of octadecanol ethylene glycol DSC (C18-SP-DSC)

C18-DSC (4.6 g, 0.0112 mol) was weighed out and placed in a sealed round bottom flask. The lipid was dissolved in anhydrous THF (100 mL) and the solution cooled down to 0°C in an ice bath. 2-(2-Aminoethoxy)ethanol (2.18 g, 0.0194 mol) and Et_3N (3.39 g, 0.0194 mol) were added to the solution which was allowed to warm to room temperature (ca. 20 °C) and then left to react overnight (16 h.). The resulting suspension was filtered to remove solids and volatiles were removed under reduced pressure. The residue was dissolved in 100 mL of DCM and the solution was washed several times with 1M HCl which was followed by several washes with brine. The organic phase was dried using anhydrous sodium sulfate ($NaSO_4$) and the DCM removed under reduced pressure. C18-ethylene glycol was recovered as a white powder (4.4 g, 98% yield).

^{1}H NMR ($CDCl_3$, 400 MHz): δ 5.23 (broad, 1H), 4.07-4.04 (t, 2H), 3.76-3.74 (t, 2H), 3.60-3.57 (m, 4H), 3.40-3.39 (t, 2H), 2.49 (broad, 1H), 1.61-1.60 (m, 2H), 1.44-1.12 (m, 30H), 0.91-0.87 (t, 3H). ^{13}C NMR ($CDCl_3$, 100 MHz): δ 156.96, 72.25, 70.22, 65.14, 61.72, 40.77, 31.92, 29.69-29.31 (multiple signals), 22.68, 14.10.

C18-ethylene glycol (4.3 g, 0.011 mol) was dissolved in anhydrous THF (100mL) and the solution cooled down to 0°C in an ice bath. DSC (5.48 g, 0.021 mol) and Et_3N (2.71 g, 0.027 mol) were added to the solution which was allowed to warm to room temperature (ca. 20 °C) and

then left to react overnight (16 h.). The resulting suspension was filtered to remove solids and volatiles were removed under reduced pressure. ^{1}H NMR analysis of the crude product revealed that only 50% of the free alcohol had reacted. Consequently, the crude product was dissolved in anhydrous THF (100 mL) and the solution cooled down to 0 °C in an ice bath. Another 1.5 eq. of DSC (4.0g, 0.015 mol) and 2.5 eq. Et3N (2.71g, 0.027 mol) added to the solution which was allowed to warm to room temperature (ca. 20 °C) and then left to react for a further 48h. The reaction mixture was passed through a short silica column (diethyl ether eluent) and the eluent subsequently removed under reduced pressure. The product was dissolved in a minimal amount of DCM and then precipitated from methanol. The product was recovered as a white powder (1.4g, 26% yield).

^{1}H NMR ($CDCl_3$, 400 MHz): δ 5.17 (broad, 1H), 4.48-4.45 (t, 2H), 4.07-4.00 (t, 2H), 3.75-3.71 (t, 2H), 3.58-3.53 (t, 2H), 3.41-3.34 (t, 2H), 2.84(s, 4H), 1.64-1.54 (m, 2H), 1.37-1.19 (m, 30H), 090-0.85 (t, 3H). ^{13}C NMR ($CDCl_3$, 100 MHz): δ 168.62, 156.93, 51.67, 70.44, 69.84, 68.16, 65.04, 50.70, 40.73, 31.90, 29.67-29.33 (multiple signals), 25.45, 22.66, 14.09. MS (ESI+) Expected m/z = 542.36; found m/z = 542.41.

Synthesis of tetradecanol-DSC (C14-DSC)

1-Tetradecanol (1 g, 0.0047 mol) was weighed out and placed in a sealed round bottom flask. The lipid was dissolved in anhydrous THF (100 mL) and the solution cooled down to 0°C in an ice bath. DSC (2.99 g, 0.012 mol) and Et_3N (1.62 g, 0.012 mol) were added to the solution which was allowed to warm to room temperature (ca. 20°C) and then left to react overnight (16 h.). The resulting suspension was filtered to remove solids and volatiles were removed under reduced pressure. C14-DSC was precipitated from water, collected by filtration, re-dissolved in THF and precipitated in water again. This procedure was repeated twice. C14-DSC was finally dissolved

in DCM and dried over $MgSO_4$ before filtration, removal of solid and evaporation of DCM under reduced pressure. C14-DSC was subsequently recovered as a white powder (1.2g, 75% yield, >85% purity, unreacted tetradecanol (<15%) present after purification).

^{1}H NMR ($CDCl_3$, 400 MHz): δ 4.32-4.28 (t, 2H), 2.82 (s, 4H), 1.76-1.69 (m, 2H), 1.42-1.18 (m, 22H), 0.89-0.84 (t, 3H). ^{13}C NMR ($CDCl_3$, 100 MHz): δ 168.73, 151.60, 71.68, 63.06 (alcohol), 31.91-28.36 (multiple signals), 25.46, 25.41, 22.68, 14.11.

Synthesis of oleyl alcohol-DSC (C18:1-DSC)

1-Oleyl alcohol (1 g, 0.0032 mol) was weighed out and placed in a sealed round bottom flask. The lipid was dissolved in anhydrous MeCN (100 mL) and the solution cooled down to 0°C in an ice bath. DSC (2.02 g, 0.0079 mol) and Et_3N (1.10 g, 0.079 mol) were added to the solution which was allowed to warm to room temperature (ca. 20°C) and then left to react overnight (16 h.). The resulting suspension was filtered to remove solids and volatiles were removed under reduced pressure. The product was extracted into hexane, insoluble material removed by filtration and volatiles removed under reduced pressure. C18:1-DSC was isolated as a yellowish oil (0.6 g, 46% yield, >92% purity).

^{1}H NMR ($CDCl_3$, 400 MHz): δ 5.40-5.30 (m, 2H), 4.33-4.29 (t, 2H), 2.83 (s, 4H), 2.05-1.93 (m, 4H), 1.78-1.70 (m, 4H), 1.42-1.20 (m, 22H), 0.90-0.85 (t, 3H). ^{13}C NMR ($CDCl_3$, 100 MHz): δ 168.69, 151.61, 129.99, 129.76, 71.67, 31.90-27.18 (multiple signals), 25.47, 25.42, 22.68, 14.11.

Oligonucleotide conjugations – Generic protocol

ODN A (5'-taa cag gat tag cag agc gag g-3', 5'-Modification: Aminolink C6) or ODN B (5'-cct cgc tct gct aat cct gtt a-3', 5'-Modification: Aminolink C6) was dissolved in isotonic PBS pH 7.4 (2.5 mg/mL) and subsequently transferred to a 15 mL Falcon tube. The DSC alkyl chain was

dissolved in THF (0.7 mg/mL, 5 eq. to the ODN) and added to ODN solution. The mixture was allowed to react for 72 h. at room temperature. Conjugate formation was monitored by HPLC. After 72 h. the THF was removed under reduced pressure and the aqueous solution concentrated. The remaining solution was transferred to a 1.5 mL Eppendorf tube and centrifuged in order to remove insoluble free alkyl chains. The alkyl-ODN conjugate was subsequently purified by semi-preparative HPLC and lyophilized. Lyophilized ODN was resuspended in DNase free water (1 mL) and the recovery estimated from the optical density at 260 nm, the solution was subsequently aliquoted into sterile Eppendorfs and lyophilized. The purified ODN-conjugates were analysed using HPLC and MALDI-TOF analysis.

Oligonucleotide Oregon Green (OG) conjugation

ODN B (5'-cct cgc tct gct aat cct gtt a-3', 5'-Modification: Aminolink C6) was dissolved in isotonic PBS pH 7.4 (2.5 mg/mL, 2.5 mL, 0.93mmol) and subsequently transferred to a 15 mL falcon tube. Oregon Green 488 Carboxylic Acid, Succinimidyl Ester (OG488) was dissolved in anhydrous DMSO at a concentration of 5 mg/mL for the fluorophore. A sample (0.5 mL) of the fluorophore solution (2.5 mg, 4.6 mmol) was added to the ODN solution and allowed to react at room temperature for 2 days. The reaction was monitored by HPLC. After 2 days the DMSO was removed using a PD-10 Desalting Column (gravity protocol), the aqueous solution was concentrated under reduced pressure and the OG-ODN conjugate purified by semi-preparative HPLC. Lyophilized OG-ODN was resuspended in DNase free water (1 mL) and the concentration calculated from the UV absorbance at 260/494 nm according to Life Technologies guidelines. Extinction coefficient of OregonGreen488 at 494nm: 80.000 (cm^{-1} M^{-1}). AbsODN = Abs260 – (AbsOG(@494nm) × 0.31). After DNA annealing the molar ratio of Oregon Green to DNA was determined by dividing the concentration of dye by the concentration of the dsDNA.

The solution was subsequently aliquoted into sterile Eppendorfs and lyophilized. The purified OG-ODN conjugate was analyzed using HPLC and MALDI-TOF analysis.

Oligo[a]	Conjugate	OD recovery[b]	Yield	MALDI[c]
A	C14	57.8	34.6%	7278/7322
A	C18	64.6	38.7%	7335/7447
A	C18:1	84.7	50.8%	7333/7359
A	C18-SP	67.2	33.6%	7410/7447
B	OG488	80.3	38.9%	7187/7367

Table 1. Analytical summary for the alkylation of oligonucleotides. a Sequences. Oligo A: TAA CAG GAT TAG CAG AGC GAG G; Oligo B: CCT CGC TCT GCT AAT CCT GTT A. b calculated from measured OD values. c theoretical/found.

Hybridization of DNA strands

Strands were hybridized in annealing buffer which consisted of 10 mM Tris, 50 mM NaCl and 1 mM EDTA pH 7.5. For the hybridization the strands were mixed in equimolar quantities to give a final concentration of ~75 µM of each strand and placed in a water bath at 95°C for 5 minutes. The water bath was then turned off and allowed to cool down to room temperature. The annealed strands were desalted using a PD SpinTrap G-25 column (gravity protocol), oligonucleotide concentration was measured using optical density at 260 nm (1 OD = 30 ug/mL). Annealing was verified using PAGE analysis. The oligonucleotide solutions were then aliquoted, lyophilized and kept in freezer before usage.

dsODN	Strand A	Strand B	OD used	OD recovery
Unmodified	ODN A	ODN B	91	81%
C14-dsODN	C14-A	ODN B	5	65%
C18-dsODN	C18-A	ODN B	24	77%
C18:1-dsODN	C18:1-A	ODN B	14	63%
C18-SPACER-dsODN	C18-SPACER-A	ODN B	16	60%
Unmodified-OG	ODN-A	OG488-B	23	77%
C18-dsODN-OG	C18-A	OG488-B	6	68%

C18-SPACER-dsODN-OG	C18-SPACER-A	OG488-B	14	50%

Table 2. Hybridization of oligonucleotide strands.

Polyacrylamide gel electrophoresis (PAGE)

Polyacrylamide gel electrophoresis (PAGE) analysis was carried out at 180 mV using a 15% acrylamide running gel. Native gels were prepared using acrylamide–bis-acrylamide (29:1) and TBE (Tris-borate-EDTA) solutions. Samples were prepared by dilution in native loading buffer containing glycerol and bromophenol blue. Quantities (5 µg) representing equivalence of each oligonucleotide was loaded per well. In instances where human serum albumin was used, 2 molar equivalents of the protein were added to the dsODN. IDT Oligo Length Standard 10/60 was used a size marker for the gels. The oligonucleotide/polymer bands were visualized using methylene blue staining.

Affinity of doxorubicin HCl to hybridized oligonucleotide strands

Fluorescence spectroscopy method[19] was used to assess the binding affinity of doxorubicin HCl to the double stranded oligonucleotide and to determine if the polymer conjugations affected the binding affinity. The assay was carried out by keeping doxorubicin HCl concentration constant at 1.5 µM throughout while the oligonucleotide was titrated from 0 to 15 molar equivalents relative to the drug. (ODN concentrations: 15, 10, 7.5 ,4.5, 1.5, 0.75, 0.45, 0.15, 0.045, 0.015, 0.005 and 0 µM). A Hill plot was used to determine the binding affinity of the double stranded oligonucleotide sequence to doxorubicin HCl (Y: (F_0-F), X: Concentration ODN µM).

Surface plasmon resonance analysis

Surface plasma resonance (SPR) analysis was carried out on a Biacore 3000 instrument using a CM5 chip. Activation and immobilization were performed at a flowrate of 10 µL/min. Activation was done using a solution of 0.2 M EDC/0.05 M NHS (1:1 mixture). Human serum albumin

(fatty acid free) was dissolved in 10 mM sodium acetate pH 5.2 and diluted to a concentration of 50 µg/mL. The albumin was immobilized at 1000 RU on the test channel and subsequently capped with 1 M ethanolamine pH 8.5; the reference channel was capped with 1 M ethanolamine pH 8.5. HBS-P was used as the eluent for the analysis. Test compounds were injected at a flowrate of 20µL/min over a 2 minute period and allowed to dissociate in HBS-P for 12 minutes. C18-dsODN, C18:1-dsODN and C14-dsODN were measured across a concentration range from 28 µM to 0 M. C18-SP-dsODN was measured from 28 µM down to 0 µM. Affinity constants were determined using the BiaEvaluation Software.

Stability of oligonucleotides

The hybridized oligonucleotide strands were incubated at an oligonucleotide concentration of 0.83 µg/mL in phosphate buffer saline containing 20 % fetal calf serum (FCS). The stability of unmodified dsODN was compared to that of alkyl conjugated ODN strands. Solutions were incubated in a water bath at 37 °C with mild agitation. Samples were taken for each oligonucleotide at 0, 24, 48 and 72 h. respectively. At each time point 9 µL samples were taken. The samples were rapidly cooled using liquid nitrogen and kept in a freezer at -20 °C until analysis by gel electrophoresis. The strands were separated on a 15% non-denaturing acrylamide gel. The samples were diluted with 12 µL of native loading buffer. An aliquot (9 µL) of the diluted sample was loaded per well, each sample was loaded in duplicate. PAGE was carried out at 160 mV. The oligonucleotide/polymer bands were visualized using methylene blue. Stability of the unmodified and C18 modified strands was determined by comparing the intensity of the ODN bands to the ODN intensity at T_0 (100%). Stability of the C18-SP-DsODN was estimated from T_{48} (100%) since it was fully protein bound before 48 h (no free dsODN or DNA fragments were observed in the gel for the C18-SP-dsODN modification while the stable complex did not

penetrate the gel fully). The ratio of albumin to dsODN in the gel was determined by comparing the intensities of the unmodified dsODN band to the albumin band at T_0. This value was used to calculate the percentage of bound dsODN in the gel for each time point. It was assumed that the binding of the alkylated dsODN to the albumin did not affect the protein staining and that protein denaturation was minimal over the course of the experiment. Band intensity was estimated using the graphical analysis software GelQuantNet.

Competitive binding assay

Solutions of C18-dsODN and C18-SP-dsODN (92 µM) were prepared in isotonic PBS. Palmitic acid solution 20 µg/µL was prepared in absolute ethanol and subsequently diluted with isotonic PBS (210-fold) to obtain a 371 µM palmitic acid stock. An equimolar quantity of albumin (185 µM) was added to the dsODN solution along with 1.25, 1.5, 1.75, 2.0 and 2.5 molar equivalent of palmitic acid. The solutions were allowed to equilibrate for 30 minutes and then analysed by aqueous SEC in order to determine the displacement for each dsODN conjugate by palmitic acid. The degree of displacement was determined by comparing the height of the dsODN (unbound) peak in absence of albumin to the dsODN (unbound) peak in presence of albumin/palmitic acid.

Melting temperature analysis of dsODNs

Thermal stability analysis of dsODN (T_m analysis) was carried out using a Beckman DU 800 UV/Vis Spectrophotometer with a Peltier Temperature Controller. UV absorbance was recorded at 260nm. The dsODNs were heated from 20 °C to 85 °C using a temperature gradient of 1°C/min and UV readings were recorded every 0.5 °C. dsODN melting point was determined by first derivative analysis of the graph. The dsODNs were dissolved in isotonic PBS pH 7.4, a dsODN concentration of ~12 µg/mL was used for the analysis.

Cell culture

MCF-7 cells were obtained from ATCC. Cells were routinely maintained in complete medium (RPMI-1640, 2 mM L-glutamine, 10% FCS) at 37 °C in 5 % CO_2. For confocal microscopy analysis, cells were seeded at 20,000 cells per well in Nunc LabTekII coverglass 8 well plates and incubated for 24 h. in complete medium. Conjugates were incubated with doxorubicin at 10% (w/w) for 30 min. at room temperature in PBS. Media (MEM, 10% FCS, 2 mM L-glutamine, 10 µg/L dNTP) was added to give a final concentration of 3 µM doxorubicin, and incubated at room temperature for 30 min. Conjugates were added to cells for the stated times. Lysosomal staining was conducted using CytoPainter Lysosomal staining kit – blue (Abcam, ab112135) following the manufacturer's instructions with an incubation time of 20 minutes. Cells were imaged immediately by LSCM using settings excitation 405 nm, emission 430−480 nm and excitation 532 nm, emission 553−672.

Mitochondria and rab5a colocalization

Cells were seeded on coverslip glass as described above. After 24 h., cells were infected with CellLight® Lysosome-RFP, ER-RFP, Early Endosome-RFP or Mitochondria-RFP (Molecular Probes). After a further 24 h. the media was removed and the cells incubated in MEM, 10% FCS, 2 mM L-glutamine, 10 ug/L dNTP for 10 minutes. Oregon green conjugates were diluted in media to a final concentration of 3 µM doxorubicin, incubated at room temperature for 30 minutes and added to cells for the stated time. Cells were fixed in fresh 4% PFA in PBS at room temperature for 10 minutes. Prolong gold antifade (Molecular probes) (10%) was added to PBS and used as a liquid mounting/imaging media. Samples were imaged by laser scanning confocal microscopy within 24 h.

Cytotoxicity assay

Cells were seeded in 96 well plates at 7,000/well in complete media. Cells were incubated with the doxorubicin-loaded conjugates for 72 hours. After this time a rezasurin cell viability assay was conducted.[26] Briefly, Rezasurin solution was added to the media to a final concentration of 60 μM then incubated for 1 h. at 37 °C. The fluorescence was measured using a Molecular Devices Flexstation 3 plate reader (λ_{ex} = 585 nm, λ_{em} = 610 nm).

Uptake assays

Cells were seeded in 96 well plates in complete media at 10,000 cells/well. Doxorubicin loaded conjugates were prepared as described above and diluted to 3 μM DNA in MEM dNTP media then incubated for the stated time. Cells were washed thrice in PBS then doxorubicin or Oregon green fluorescence was measured using Molecular Devices Flexstation 3 plate reader.

RESULTS AND DISCUSSION

Synthesis of alkylated dsODNs

Alkylated ODN conjugates were synthesized by adopting the method we have previously described for the PEGylation of ODNs.[20,27] Alkyl alcohols were activated using *N*,*N*-disuccinimidyl carbonate to form amino-reactive alkyl-succinimidyl carbonates (ASC). The activated alkyl derivatives were conjugated to the 5' end of amine modified ODN (Oligo A: TAA CAG GAT TAG CAG AGC GAG G) (Figure 1b). The oligonucleotide sequence and its complementary sequence were chosen on their ability to form a strong physical complex with doxorubicin as a dsODN.[20] The reaction was carried out in a 1:1 solution mixture of THF/PBS with an excess (>5 eq.) of the activated alkyl chain. Initial conjugations and screening were carried out for tetradecanol (C14), octadecanol (C18) and 3 cis-9-octadecenol (C18:1). For uptake/co-localization studies the 5' C6 amine-modified complementary strand (Oligo B: CCT

CGC TCT GCT AAT CCT GTT A) was conjugated to NHS Oregon Green 488 (OG488) (Figure 1c). The reactions were monitored using HPLC and then purified by semi-preparative HPLC. All of the alkylation reactions achieved >95% conversion relative to the amine modified ODN. However, the reaction between NHS OG488 and the complementary strand achieved ~50% conversion due to the rapid hydrolysis of the activated NHS ester under the synthetic conditions. Alkylated and fluorophore-modified ODNs were purified by HPLC and recovered in moderate yield (35–50%). Low recovery after purification was attributed to the losses during sample preparation/filtration due to the low sample volumes.

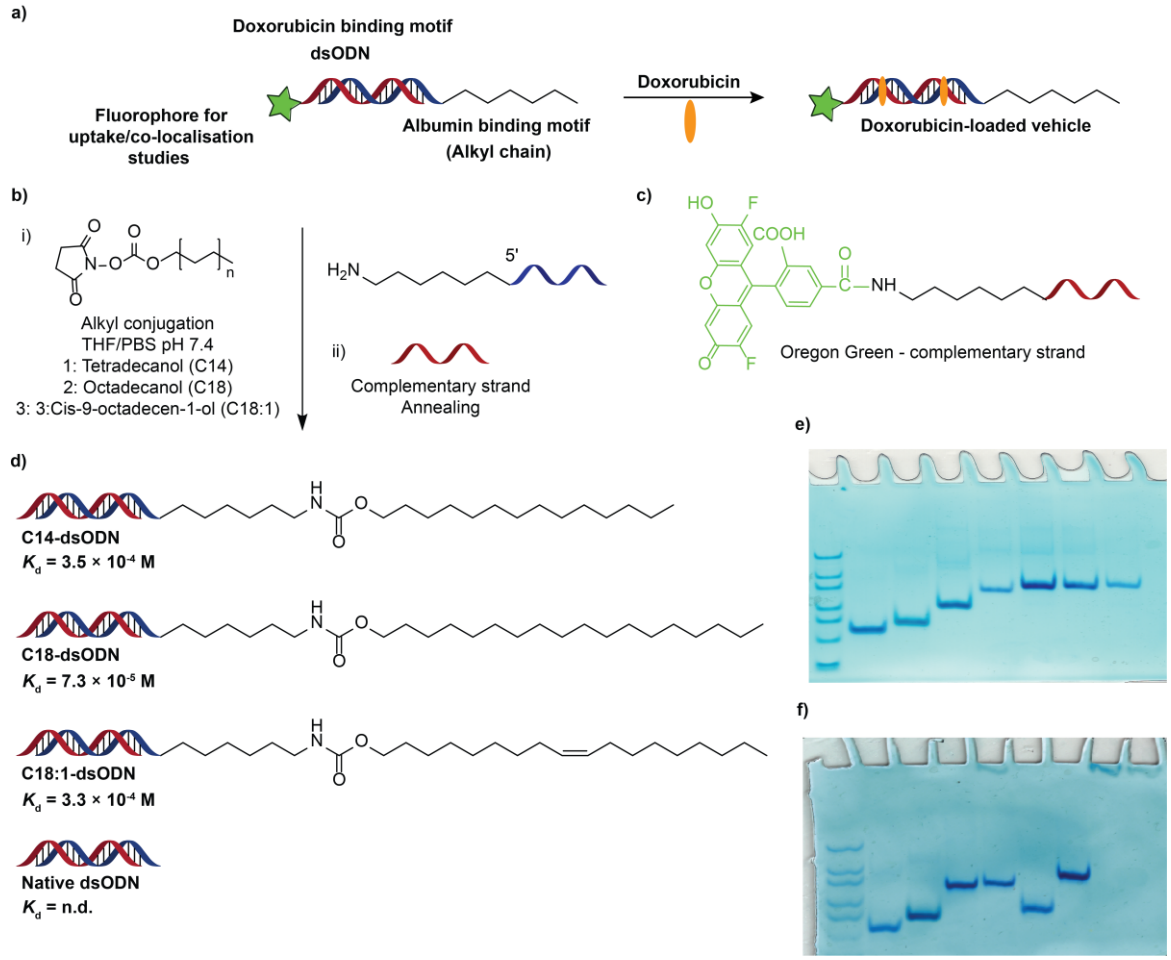

Figure 1 – a) Schematic representation of the dsODN alkyl design utilized for enhanced delivery of doxorubicin and uptake /co-localization studies of the oligonucleotide carrier. b) Conjugation

of alkyl derivatives to main strand (5' C6-amine) i) Conditions of conjugation and alkyl derivatives coupled ii) hybridization with unmodified complementary strand c) Complementary strand Oregon Green conjugate (5' C6-amine modification). d) dsODN-alkyl derivatives synthesized and their albumin equilibrium dissociation constant derived by SPR analysis. e) PAGE analysis of dsODN-alkyl Oregon Green derivatives. (1) IDT Ladder10/60, (2) ODN A, (3) ODN B, (4) ODN B– OG488, (5) dsODN– OG488, (6) C14 – dsODN – OG488, (7) C18:1 – dsODN – OG488, (8) C18 – dsODN – OG488. f) PAGE analysis of C18-dsODN derivative. (1) IDT Ladder10/60, (2) ODN A, (3) ODN B, (4) dsODN, (5) dsODN + Albumin, (6) C18 – ODN A (7) C18 – dsODN, (8) C18 – dsODN + Albumin, (9) Albumin only.

The purity of the modified ODNs was determined by HPLC and polyacrylamide gel electrophoresis (Figures S1/S2 and 1e and 1f) and the identity of the desired products confirmed by MALDI-TOF mass spectrometry (Table 1). Alkylated ODN strands were annealed with unmodified complementary DNA to form a series of monoalkylated dsODN. PAGE analysis of the annealed strands confirmed that no free strand(s) were present after annealing (Figure 1e and 1f). In order to confirm that albumin was able to bind monoalkylated-dsODN, PAGE analysis was performed in the presence of HSA. The C18-dsODN was completely bound to the albumin while the unsaturated C18:1 and C14 modified dsODNs were only partially bound under these conditions (Figure 1f). As expected, no binding was observed for the unmodified dsODN to albumin.

Albumin-binding of alkylated dsODNs

The disassociation constants (K_D) for the alkyl-dsODN albumin complexes were determined by surface plasmon resonance (SPR) analysis. The surface of an SPR chip (CM5) was modified

with albumin using standard EDC/NHS coupling chemistry. Samples containing a range of concentrations of the alkyl-dsODNs were injected over the albumin modified surface and the disassociation constants determined by the SPR response (Figure S3). Curve fitting was performed assuming 1:1 stoichiometry, because the large size of the dsODN, ~7.5 nm length and ~2 nm diameter,[28] is expected to prevent multiple binding to albumin. Analysis by dynamic light scattering supported this assumption with no increase in complex size observed at higher alkyl-dsODN to albumin ratios and an average hydrodynamic diameter of 9 nm for both complexes (Figure S4). The C18 derivative formed the highest affinity complex with albumin out of the three alkyl-dsODN conjugates. No binding response was observed for unmodified, "native" dsODN. Based on these results the C18-dsODN derivative was selected for further studies and optimization while the C14 and the unsaturated C18 derivatives were omitted from further testing based on their weaker albumin binding.

The crosslinking chemistry, and more importantly the length of linker, can play a pivotal role in determining the activity of a crosslinked macromolecular conjugate.[29] We hypothesized that the large size of dsODN (~7.5 nm length and ~2 nm diameter)[28] and close vicinity of the fatty acid moiety to the dsODN strand could have great impact on its affinity to albumin. Consequently, a small spacer was placed between the alkyl chain and the ODN of the C18-dsODN conjugate and its effects examined (Figure 2a). A diethylene glycol based linker, 2-(2-aminoethoxy)ethanol was conjugated to the C18 DSC-activated chain and the resulting free hydroxyl was activated again using DSC to produce the amine reactive C18-Spacer (C18-SP). The C18-SP derivative was synthesized, purified and characterized as described for the previous alkyl-ODN derivatives.

The albumin binding of the two conjugates was compared using a competitive displacement assay. Albumin and each alkyl conjugate were mixed in a 1:1 molar ratio and equilibrated for 30 min. Complex formation was validated by size exclusion chromatography (SEC). Palmitic acid (1.25 eq, 1.75 eq and 2.5 eq.) was added to the complexes and the solution equilibrated for 30 minutes. After equilibration, the displacement of the albumin-alkyl dsODN complex by palmitic acid was subsequently determined by SEC (Figures 2b and S5). The displacement assay confirmed that introduction of the spacer significantly improved the albumin binding. Around 35% of the C18-dsODN conjugate was displaced from albumin at the highest concentration of palmitic acid tested while in the case of the C18-SP-dsODN only 20% was displaced.

The stability of the two C18 dsODN conjugates and the unmodified dsODN were examined in presence of fetal calf serum over a period of 72 h. by PAGE analysis and quantified using image analysis (Figures 2c and S6).

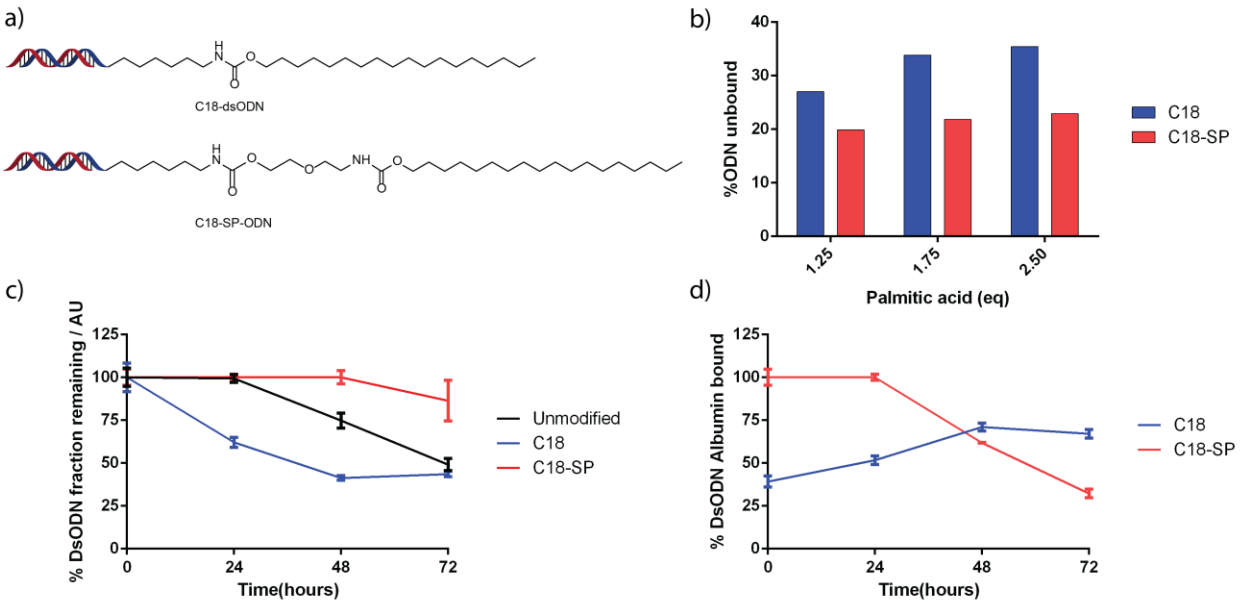

Figure 2 – a) Structure of alkyl derivatives evaluated against unmodified dsODN and free drug in vitro: C18-dsODN and C18-SP-dsODN. b) Competitive displacement of alkyl-dsODN

albumin (1:1) complex with increasing equivalents of palmitic acid as determined by size exclusion chromatography. c) and d) Stability of dsODN derivatives in presence of serum.

In this experiment, the C18-SP-dsODN was the most stable of three dsODN constructs with ~87% remaining intact after 72 h. C18-dsODN and unmodified dsODN were both degraded more quickly with ~45% of each dsODN remaining after 72 h. The stability study also suggests that the initial degradation of the C18-dsODN was faster than that of the unmodified dsODN. Examination of the PAGE gels (Figure S6) used to determine DNA stability revealed a difference in albumin binding between the two C18 derivatives. The C18-SP-dsODN derivative largely remained albumin-bound for the first 48 h. and showed limited degradation. In contrast, the C18-dsODN derivative was only 40% albumin bound at the start of the experiment and therefore more rapidly degraded due to lower steric hindrance and thus higher accessibility to nucleases. The increased degradation observed for the C18-dsODN compared to the unmodified dsODN is not fully understood, but it is plausible that ODN-nuclease hydrophobic interactions are enhanced by the alkyl chain when it is not bound to the albumin.[30]

The affinity of doxorubicin to the dsODN conjugates was determined by a fluorescence quenching protocol.[19] The affinity of doxorubicin to the dsODN was slightly enhanced by modification with alkylated dsODNs displaying slightly lower dissociation constants to the unmodified dsODN (Figure S7, K_D = 110 ± 30 nM vs. 217 ± 91 nM).[20]

Alkyl-modified dsODN uptake studies

The C18-dsODN, C18-SP-dsODN and unmodified dsODN were compared using *in vitro* cell-based assays to determine their uptake characteristics and ability to deliver doxorubicin efficiently into resistant cells. To assess cellular uptake, Oregon Green-labelled dsODNs were incubated with MCF-7 cells for 4 hours prior to quantification of cell-associated fluorescence levels (Figure 3a)

and visualization by confocal microscopy in cells modified with fluorescently labelled organelle markers (Figure 3b). Unmodified dsODN was taken up at significantly lower levels than either alkyl-modified ODNs while the high affinity albumin binding variant dsODN-Spacer-C18 uptake was significantly (1-way ANOVA, $p<0.01$) higher than the C18 derivative (Figure 3a). Microscopy revealed partial colocalization of alkyl-modified conjugates with both the early endosome marker Rab5a and the mitochondria (Figure 3b). Due to the highly charged and hydrophilic nature of the oligonucleotides, internalization of these particles is unlikely to occur by diffusion or 'flip-flop' across the plasma membrane as is common with fatty acid uptake.[31] Instead an active endocytic pathway is likely. Both albumin and fatty acids are known to be internalized into cells via multiple pathways. Albumin has been shown to be readily internalized via pinocytosis into Rab5 positive endosomes.[32–34] Therefore, due to the conjugates' high affinity for albumin and colocalization demonstrated in figure 3b this is a potential route of entry. Fatty acids have also been demonstrated to be internalized by fatty acid translocase CD36 via a novel, poorly defined endocytic pathway.[35,36] Once internalized fatty acids are known to traffic effectively to the mitochondria where they provide a high energy source for the cell.[37,38] Our data suggests that alkyl modification of DNA allows rapid cellular internalization of the complex with a proportion trafficking via Rab5a early endosomes and results in targeting of short DNA sequences to the mitochondria. Uptake studies were also performed in A549 cells and the results were consistent with MCF-7 cells (Figure S10).

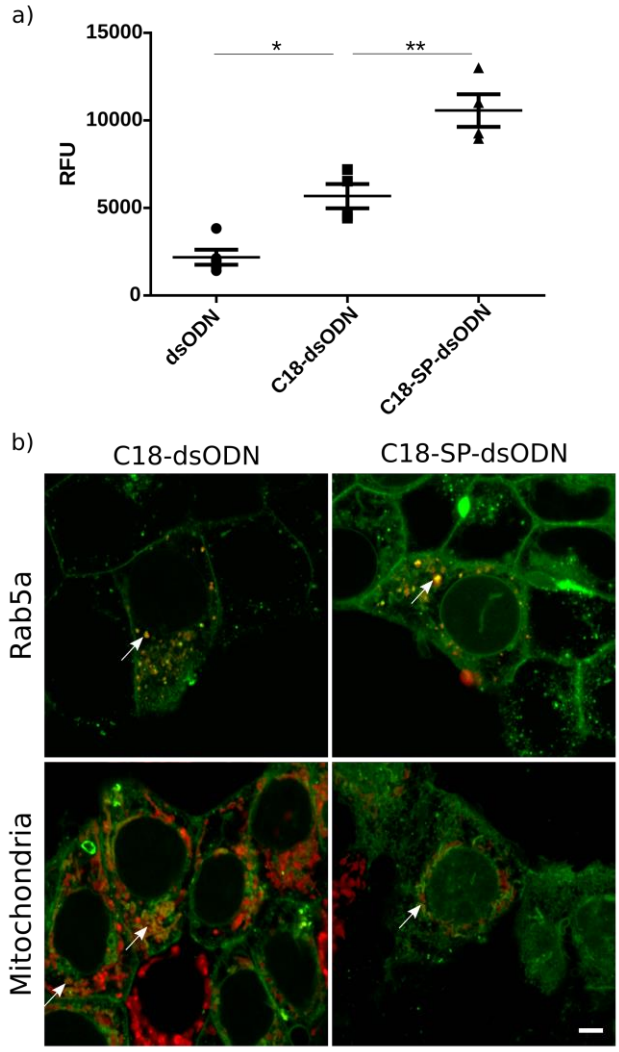

Figure 3 – Alkyl-modified dsODN are rapidly internalized. a) Cells were incubated with Oregon Green-labelled dsODN and fluorescence measured after 4 hours. Mean ± SEM; RFU = relative fluorescence units. One-way ANOVA * $p < 0.05$, ** $p < 0.01$. b) Oregon Green-labelled dsODN were incubated with cells labelled for Rab5a or the mitochondria using CellLight BacMam system. After 4 hours the cells were visualized by confocal microscopy. Oregon Green (Green), mitochondria/Rab5a (red). Arrows show areas of colocalization. Scale bar = 5 µm.

Linker structure determines cellular uptake and localization.

To understand further the cellular update and localization, doxorubicin-loaded dsODNs were incubated with cells for 4 h., after which time the lysosomes were counterstained and the inherent fluorescence of doxorubicin used to visualize drug location by confocal microscopy (Figure 4). Both free drug and C18-SP-dsODN demonstrated high levels of doxorubicin localization in the nucleus and punctate cytoplasmic regions. C18-SP-dsODN cytoplasmic staining colocalizes with a lysosomal marker. Cells incubated with doxorubicin lacked clear lysosomal staining. This is likely due to doxorubicin lysosomal trapping resulting in exclusion of lysosome stain from the organelle.[39,40] Unmodified and C18-dsODN showed considerably lower levels of doxorubicin fluorescence at 4 hours with localization largely confined to the lysosome and cytoplasm. At 18 h. this pattern is maintained with C18-SP-dsODN and free drug having higher levels of doxorubicin by both microscopy (Figure 5a) and quantification of innate doxorubicin fluorescence (Figure 5b). Unmodified and C18-dsODN fluorescence levels remain significantly lower albeit with nuclear localization.

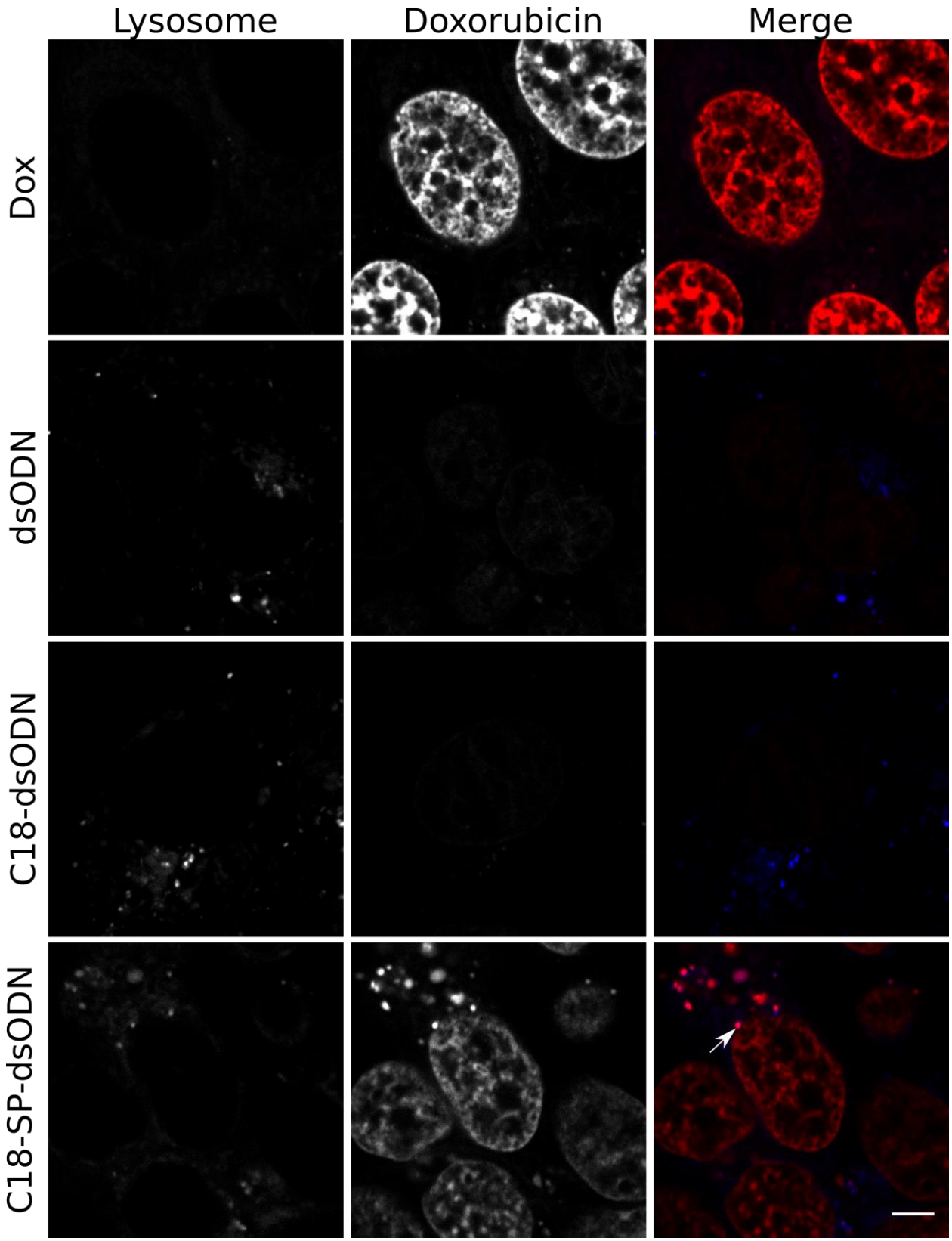
Lysosome
Doxorubicin
Merge
Dox
dsODN
C18-dsODN
C18-SP-dsODN

Figure 4 – Alkyl-modified C18-SP dsODN delivers doxorubicin to the nucleus. Cells were incubated for 4 hours with Dox loaded dsODNs at a concentration equivalent to 3 μM Dox. Lysosomes were counterstained with Cellpainter lysosome blue and imaged by confocal microscopy. Doxorubicin (red), Lysosome (blue). Arrows shows areas of colocalization. Scale bar = 5 μm.

Oregon Green-labelled conjugates exhibited partial colocalization with a lysosomal marker after 18 h, while no signal was detectable in the mitochondria (Figure S8). It was noted that at 18 h. both doxorubicin (Figure 5a, arrows) and Oregon Green signals (Figure S9) were detected in the cellular plasma membrane for C18-SP-dsODN treated cells but not C18-dsODN samples which exhibited a punctate cytoplasmic localization for Oregon Green staining. We suggest that the enhanced stability and resistance to degradation demonstrated by C18-SP-dsODN (Figure 2c) results in intact, labelled conjugates embedding in the membrane via standard albumin bound fatty acid trafficking pathways. In contrast, C18-dsODN samples are more sensitive to nuclease activity which results in cleavage of the terminal Oregon Green-labelled 5' nucleotides. This is then free to be taken up by fluid phase endocytosis or via specific pathways, such as Equilibrative Nucleoside Transporter,[41] resulting in uptake of label in a punctate pattern. Localisation studies were also performed in A549 cells and the results were consistent with MCF-7 cells (Figures S11 and S12).

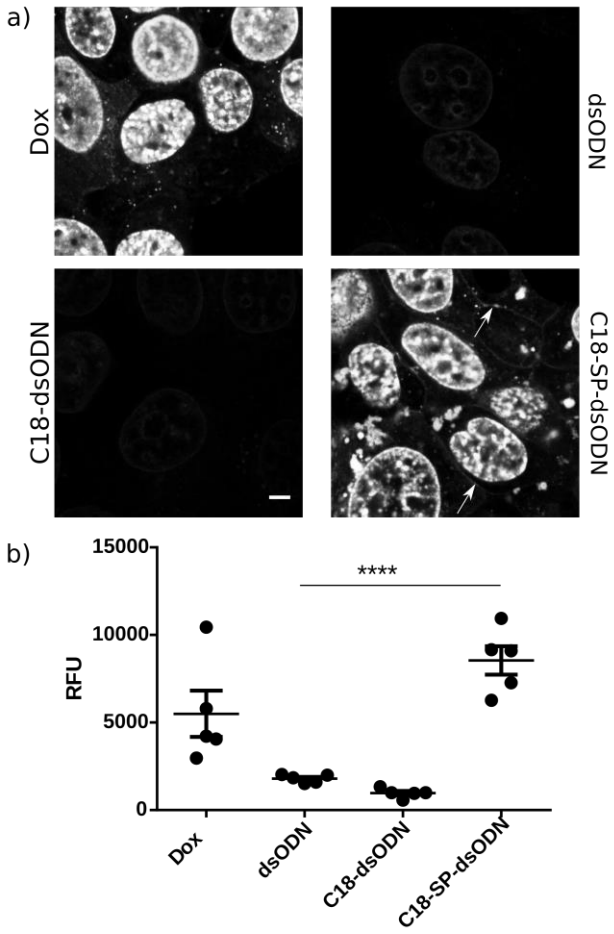

Figure 5 – Doxorubicin uptake at 18 hours. a) Cells were incubated with Dox loaded dsODN for 18 hours at a concentration equivalent to 3 μM Dox then visualized by confocal microscopy. Arrows highlight membrane staining. Bar 5 μM. b) After 18 hours doxorubicin fluorescence was measured, RFU: relative fluorescence units. Mean +/- SEM, one way ANOVA **** $p<0.0001$.

Incorporation of spacer restores DOX cytotoxicity

The cytotoxicity of doxorubicin-loaded dsODNs and unloaded dsODNs carriers was investigated in MCF7 cell line over 72 h. None of the drug free carriers demonstrated cellular toxicity and cellular growth was not enhanced when the cell media was supplemented with free nucleosides (Figure 5a).[20] Free doxorubicin (IC50 200 nM) and doxorubicin loaded C18-SP-dsODN (IC50 276

nM) carrier exhibited similar dose responses while very low toxicity was observed for the unmodified and C18-dsODN drug complexes. Consequently, it can be suggested that the specific choice of linker determines the efficacy of the conjugate with respect to doxorubicin delivery and cytotoxicity. Cytotoxicity studies were also performed in A549 cells and the results were consistent with MCF-7 cells (Figures 13).

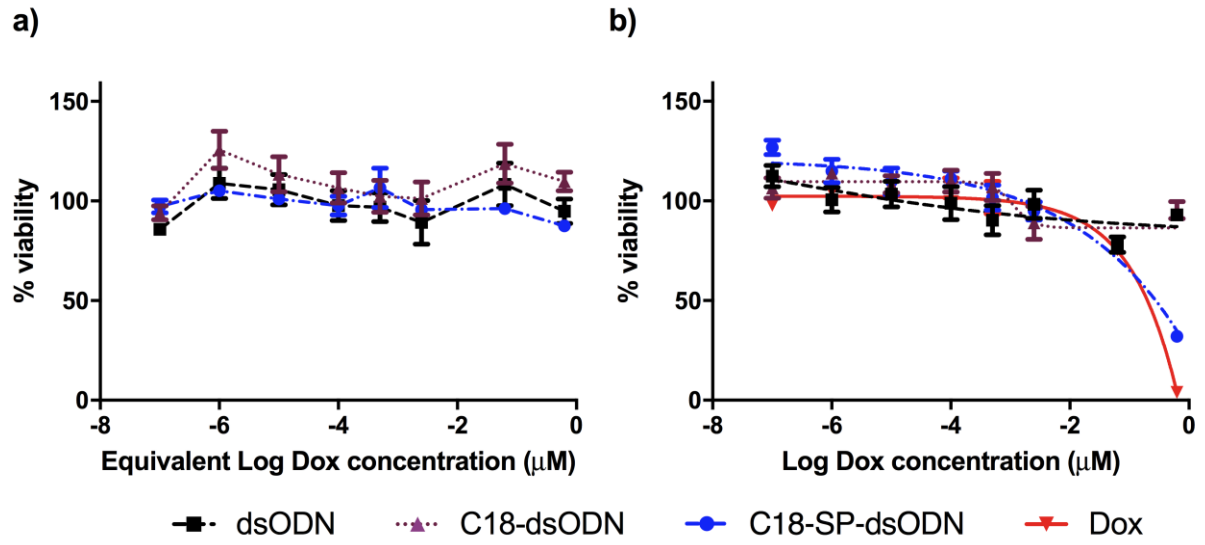

Figure 6 a) Toxicity of dsODN carriers, b) Toxicity of free doxorubicin and Doxorubicin-loaded dsODN. Viability was measured using Alamar blue assay.

In conclusion, we have demonstrated that dsODNs modified with alkyl chains are successfully internalized into cells and trafficked to the mitochondria, mimicking the natural pathway for fatty acids. Trafficking of fatty acids to the mitochondria opens the possibility to specifically deliver therapeutic moieties to the organelle to treat mitochondrial disease. We also suggest that alkyl chain modification could prove beneficial for other applications, for example in mitochondrial DNA gene editing using technologies such as Crispr/Cas9 and TALEN. Specific cleavage of mitochondrial DNA has been achieved using modified versions of both systems although gene

replacement has not yet been demonstrated.[42,43] Specific targeting of a therapeutic template DNA strand to the mitochondria during gene editing is likely to increase successful gene replacement and limit off target nuclear effects.

Incorporation of an additional spacer between the dsODN and alkyl chain (C18-SP-dsODN) increased albumin binding affinity and displayed excellent stability in serum over 72 h. Incorporation of the spacer also restored doxorubicin-cytotoxicity to comparable levels as free doxorubicin due to successful delivery to the nucleus.

Supporting Information. This material is available free of charge via the Internet at http://pubs.acs.org. Additional microscopy images and data for A549 cells. SPR traces and fitting curves. PAGE analysis of annealed strands and degradation study. ^{1}H NMR spectra. HPLC traces of purified alkyl-ODN derivatives and Oregon Green-ODN. Doxorubicin-ODN affinity plots for C18 and C18-Spacer derivatives. T_m analysis of dsODN: C18, C18-Spacer and unmodified. SEC traces for alkyl-dsODN albumin displacement assay. DLS analysis of albumin:C18-dsODN complexes.

AUTHOR INFORMATION

Corresponding Author

*Email: johannespall@gmail.com, s.g.spain@sheffield.ac.uk.

Author Contributions

LP and JPM performed all experiments. All authors contributed to experimental design. The manuscript was written through contributions of all authors. All authors have given approval to the final version of the manuscript.

Notes

The authors declare no competing financial interest.

ACKNOWLEDGMENTS

We thank the UK Engineering and Physical Sciences Research Council (EPSRC) for financial support (Leadership Fellowship to CA and Grants EP/H005625/1, and EP/J021180/1).

Data access statement

All raw data created during this research are openly available from the corresponding author (cameron.alexander@nottingham.ac.uk) and at the University of Nottingham Research Data Management Repository (https://rdmc.nottingham.ac.uk/) and all analysed data supporting this study are provided as supplementary information accompanying this paper.

ABBREVIATIONS

ODN, Oligonucleotide; dsODN, double stranded oligonucleotide; OG488, Oregon Green 488; OG, Oregon Green; SPR, Surface plasma resonance; PEG, Polyethylene glycol; ; DOX, Doxorubicin; DNA, Deoxyribonucleic acid; ODN, Oligonucleotide; IC, Inhibitory concentration; EPR, Enhanced Permeation Retention; HPLC, High performance liquid chromatography; MALDI-ToF, Matrix-assisted laser desorption/ionization time-of flight mass spectroscopy; PAGE, Polyacrylamide gel electrophoresis; Size exclusion chromatography, SEC.

REFERENCES

(1) Kotas, M. E.; Medzhitov, R. Homeostasis, Inflammation, and Disease Susceptibility. *Cell* **2016**, *160*, 816–827.

(2) Duncan, R.; Vicent, M. J. Polymer Therapeutics-Prospects for 21st Century: The End of the Beginning. *Adv. Drug Deliv. Rev.* **2013**, *65*, 60–70.

(3) Haag, R.; Kratz, F. Polymer Therapeutics: Concepts and Applications. *Angew. Chem. Int. Ed.* **2006**, *45*, 1198–1215.

(4) Farokhzad, O. C.; Langer, R. Impact of Nanotechnology on Drug Delivery. *ACS Nano* **2009**, *3*, 16–20.

(5) Hornef, M. W.; Wick, M. J.; Rhen, M.; Normark, S. Bacterial Strategies for Overcoming Host Innate and Adaptive Immune Responses. *Nat. Immunol.* **2002**, *3*, 1033–1040.

(6) Yoo, J.-W.; Irvine, D. J.; Discher, D. E.; Mitragotri, S. Bio-Inspired, Bioengineered and Biomimetic Drug Delivery Carriers. *Nat. Rev. Drug Discov.* **2011**, *10*, 521–535.

(7) Mudhakir, D.; Harashima, H. Learning from the Viral Journey: How to Enter Cells and How to Overcome Intracellular Barriers to Reach the Nucleus. *AAPS J.* **2009**, *11*, 65–77.

(8) Larsen, M. T.; Kuhlmann, M.; Hvam, M. L.; Howard, K. A. Albumin-Based Drug Delivery: Harnessing Nature to Cure Disease. *Mol. Cell. Ther.* **2016**, *4*, 1–12.

(9) Elzoghby, A. O.; Samy, W. M.; Elgindy, N. A. Albumin-Based Nanoparticles as Potential Controlled Release Drug Delivery Systems. *J. Control. Release* **2012**, *157*, 168–182.

(10) Kratz, F. Albumin as a Drug Carrier: Design of Prodrugs, Drug Conjugates and Nanoparticles. *J. Control. Release* **2008**, *132*, 171–183.

(11) Sleep, D.; Cameron, J.; Evans, L. R. Albumin as a Versatile Platform for Drug Half-Life Extension. *Biochim. Biophys. Acta - Gen. Subj.* **2013**, *1830*, 5526–5534.

(12) Sand, K. M. K.; Bern, M.; Nilsen, J.; Noordzij, H. T.; Sandlie, I.; Andersen, J. T.

Unraveling the Interaction between FcRn and Albumin: Opportunities for Design of Albumin-Based Therapeutics. *Front. Immunol.* **2015**, *5*.

(13) Frei, E. Albumin Binding Ligands and Albumin Conjugate Uptake by Cancer Cells. *Diabetol. Metab. Syndr.* **2011**, *3*, 11.

(14) Commisso, C.; Davidson, S. M.; Soydaner-Azeloglu, R. G.; Parker, S. J.; Kamphorst, J. J.; Hackett, S.; Grabocka, E.; Nofal, M.; Drebin, J. A.; Thompson, C. B.; *et al.* Macropinocytosis of Protein Is an Amino Acid Supply Route in Ras-Transformed Cells. *Nature* **2013**, *497*, 633–637.

(15) Hradec, J. Metabolism of Serum Albumin in Tumour-Bearing Rats. *Brit. J. Cancer*, 1958, *12*, 290–304.

(16) Neumann, E.; Frei, E.; Funk, D.; Becker, M. D.; Schrenk, H.-H.; Müller-Ladner, U.; Fiehn, C. Native Albumin for Targeted Drug Delivery. *Expert Opin. Drug Deliv.* **2010**.

(17) Clark, A. J.; Wiley, D. T.; Zuckerman, J. E.; Webster, P.; Chao, J.; Lin, J.; Yen, Y.; Davis, M. E. CRLX101 Nanoparticles Localize in Human Tumors and Not in Adjacent, Nonneoplastic Tissue after Intravenous Dosing. *Proc. Nat. Acad. Sci. USA.* **2016**, *113*, 3850–3854.

(18) Frederick, C. A.; Williams, L. D.; Ughetto, G.; van der Marel, G. A.; van Boom, J. H.; Rich, A.; Wang, A. H. Structural Comparison of Anticancer Drug-DNA Complexes: Adriamycin and Daunomycin. *Biochemistry* **1990**, *29*, 2538–2549.

(19) Bagalkot, V.; Farokhzad, O. C.; Langer, R.; Jon, S. An Aptamer–Doxorubicin Physical Conjugate as a Novel Targeted Drug-Delivery Platform. *Angew. Chemie Int. Ed.* **2006**, *45*, 8149–8152.

(20) Purdie, L.; Alexander, C.; Spain, S. G.; Magnusson, J. P. Influence of Polymer Size on

Uptake and Cytotoxicity of Doxorubicin-Loaded DNA-PEG Conjugates. *Bioconjug. Chem.* **2016**, *27*, 1244–1252.

(21) Setyawati, M. I.; Kutty, R. V.; Leong, D. T. DNA Nanostructures Carrying Stoichiometrically Definable Antibodies. *Small* **2016**, 1–11.

(22) Alexander, C. M.; Maye, M. M.; Dabrowiak, J. C. DNA-Capped Nanoparticles Designed for Doxorubicin Drug Delivery. *Chem. Commun.* **2011**, *47*, 3418–3420.

(23) Zhang, L.; Radovic-Moreno, A. F.; Alexis, F.; Gu, F. X.; Basto, P. A.; Bagalkot, V.; Jon, S.; Langer, R. S.; Farokhzad, O. C. Co-Delivery of Hydrophobic and Hydrophilic Drugs from Nanoparticle–Aptamer Bioconjugates. *ChemMedChem* **2007**, *2*, 1268–1271.

(24) Zhao, Y.; Shaw, A.; Zeng, X.; Benson, E.; Nyström, A. M.; Högberg, B. DNA Origami Delivery System for Cancer Therapy with Tunable Release Properties. *ACS Nano* **2012**, *6*, 8684–8691.

(25) Kim, K.-R.; Kim, D.-R.; Lee, T.; Yhee, J. Y.; Kim, B.-S.; Kwon, I. C.; Ahn, D.-R. Drug Delivery by a Self-Assembled DNA Tetrahedron for Overcoming Drug Resistance in Breast Cancer Cells. *Chem. Commun.* **2013**, *49*, 2010–2012.

(26) Ivanov, D. P.; Parker, T. L.; Walker, D. A.; Alexander, C.; Ashford, M. B.; Gellert, P. R.; Garnett, M. C. Multiplexing Spheroid Volume, Resazurin and Acid Phosphatase Viability Assays for High-Throughput Screening of Tumour Spheroids and Stem Cell Neurospheres. *PLoS One* **2014**, *9*, e103817.

(27) Magnusson, J. P.; Fernández-Trillo, F.; Sicilia, G.; Spain, S. G.; Alexander, C. Programmed Assembly of Polymer-DNA Conjugate Nanoparticles with Optical Readout and Sequence-Specific Activation of Biorecognition. *Nanoscale* **2014**, *6*, 2368–2374.

(28) Victor A. Bloomfield; Crothers, D. M.; Tinoco, I. *Nucleic Acids: Structures, Properties,*

and Function; University Science Books: Mill Valley, CA, 2001; Vol. 6.

(29) Mattson, G.; Conklin, E.; Desai, S.; Nielander, G.; Savage, M. D.; Morgensen, S. A Practical Approach to Crosslinking. *Mol. Biol. Rep. 17*, 167–183.

(30) Kim, H.-K.; Tuite, E.; Nordén, B.; Ninham, B. W. Co-Ion Dependence of DNA Nuclease Activity Suggests Hydrophobic Cavitation as a Potential Source of Activation Energy. *Eur. Phys. J. E* **2001**, *4*, 411–417.

(31) Kamp, F.; Zakim, D.; Zhang, F.; Noy, N.; Hamilton, J. A. Fatty Acid Flip-Flop in Phospholipid Bilayers Is Extremely Fast. *Biochemistry* **1995**, *34*, 11928–11937.

(32) Moldenhauer, G.; Henne, C.; Karhausen, J.; Möller, P. Surface-Expressed Invariant Chain (CD74) Is Required for Internalization of Human Leucocyte Antigen-DR Molecules to Early Endosomal Compartments. *Immunology* **1999**, *96*, 473–484.

(33) Strømhaug, P. E.; Berg, T. O.; Gjøen, T.; Seglen, P. O. Differences between Fluid-Phase Endocytosis (Pinocytosis) and Receptor-Mediated Endocytosis in Isolated Rat Hepatocytes. *Eur. J. Cell Biol.* **1997**, *73*, 28–39.

(34) Francis, G. L. Albumin and Mammalian Cell Culture: Implications for Biotechnology Applications. *Cytotechnology* **2010**, *62*, 1–16.

(35) Collins, R. F.; Touret, N.; Kuwata, H.; Tandon, N. N.; Grinstein, S.; Trimble, W. S. Uptake of Oxidized Low Density Lipoprotein by CD36 Occurs by an Actin-Dependent Pathway Distinct from Macropinocytosis. *J. Biol. Chem.* **2009**, *284*, 30288–30297.

(36) Bonen, A.; Campbell, S. E.; Benton, C. R.; Chabowski, A.; Coort, S. L. M.; Han, X.-X.; Koonen, D. P. Y.; Glatz, J. F. C.; Luiken, J. J. F. P. Regulation of Fatty Acid Transport by Fatty Acid translocase/CD36. *Proc. Nutr. Soc.* **2004**, *63*, 245–249.

(37) Kerner, J.; Hoppel, C. Fatty Acid Import into Mitochondria. *Biochim. Biophys. Acta* **2000**,

1486, 1–17.

(38) Rambold, A. S.; Cohen, S.; Lippincott-Schwartz, J. Fatty Acid Trafficking in Starved Cells: Regulation by Lipid Droplet Lipolysis, Autophagy, and Mitochondrial Fusion Dynamics. *Dev. Cell* **2015**, *32*, 678–692.

(39) Bauch, C.; Bevan, S.; Woodhouse, H.; Dilworth, C.; Walker, P. Predicting in Vivo Phospholipidosis-Inducing Potential of Drugs by a Combined High Content Screening and in Silico Modelling Approach. *Toxicol. Vitr.* **2015**, *29*, 621–630.

(40) Herlevsen, M.; Oxford, G.; Owens, C. R.; Conaway, M.; Theodorescu, D. Depletion of Major Vault Protein Increases Doxorubicin Sensitivity and Nuclear Accumulation and Disrupts Its Sequestration in Lysosomes. *Mol. Cancer Ther.* **2007**, *6*, 1804–1813.

(41) Young, J. D.; Yao, S. Y. M.; Sun, L.; Cass, C. E.; Baldwin, S. A. Human Equilibrative Nucleoside Transporter (ENT) Family of Nucleoside and Nucleobase Transporter Proteins. *Xenobiotica* **2008**, *38*, 995–1021.

(42) Bacman, S. R.; Williams, S. L.; Pinto, M.; Peralta, S.; Moraes, C. T. Specific Elimination of Mutant Mitochondrial Genomes in Patient-Derived Cells by mitoTALENs. *Nat Med* **2013**, *19*, 1111–1113.

(43) Jo, A.; Ham, S.; Lee, G. H.; Lee, Y.-I.; Kim, S.; Lee, Y.-S.; Shin, J.-H.; Lee, Y. Efficient Mitochondrial Genome Editing by CRISPR/Cas9. *Biomed Res. Int.* **2015**, *2015*, 305716.